Cement and Concrete Research 40 (2010) 477–487

Contents lists available at ScienceDirect

Cement and Concrete Research

journal homepage: http://ees.elsevier.com/CEMCON/default.asp

# Temperature, pore pressure and mass variation of concrete subjected to high temperature — Experimental and numerical discussion on spalling risk

Jean-Christophe Mindeguia [a,b,*], Pierre Pimienta [a], Albert Noumowé [c], Mulumba Kanema [c]

[a] Centre Scientifique et Technique du Bâtiment, 84 Avenue Jean Jaurès, Champs sur Marne, 77447 Marne la Vallée Cedex, France
[b] Laboratoire des Sciences Appliquées au Génie Civil et Côtier, Université de Pau et des Pays de l'Adour, Allée du Parc Montaury, 64600 Anglet, France
[c] Laboratoire de Mécanique et Matériaux du Génie Civil, Université de Cergy-Pontoise, 5 mail Gay Lussac, Neuville sur Oise, 95031 Cergy-Pontoise, France

ARTICLE INFO

*Article history:*
Received 25 June 2008
Accepted 8 October 2009

*Keywords:*
Temperature (A)
Spalling
Pore vapour pressure
Mass loss
Fire behaviour
Thermomechanical behaviour

ABSTRACT

Spalling at high temperature is a phenomenon that can be observed in different materials such as ceramics, rocks and bricks. For concrete, this phenomenon, considered as a thermal instability of the material, can seriously jeopardize the integrity of a whole structure during fire and can even constitute a risk for people. Many explanations to the spalling risk exist but still no model can accurately predict it. Among them, models based on thermo-hydral behaviour of concrete have been proposed and developed by several authors. In particular, an important role is given to the pore vapour pressure, considered by many authors as the main mechanism for the trigger of such a thermal instability. However, pore vapour pressure is not easy to measure and numerical works still need more experimental results to validate their assumptions regarding the spalling risk. This paper presents the results of an experimental study carried out on five different concrete mixtures. We used a device intended for measuring temperature, pore vapour pressure and mass loss of concrete specimens. The aim of the study was to better understand the thermo-hydral behaviour of concrete exposed to high temperature and the possible link to spalling risk. In particular, we focused on the influence of matrix compactness on the transfer properties of concrete and we discussed about the importance of pore vapour pressure on spalling risk. Moreover, based on our experimental observations, a numerical analysis of the influence of water content on the thermomechanical behaviour of concrete during heating is done.



## 1. Introduction

Concrete structure design must take into account the risk of temperature increase. Heating can be caused by fires (in tunnels, high rise buildings, underground parks…) or by accidental situations in nuclear power plants (e.g. LOCA, loss of coolant accident or contact between liquid sodium and the steel liner of the concrete reactor vessel). Concrete behaviour at high temperature is very complex and influences the global behaviour of a structure during heating. Particularly, previous studies have shown the important risk of thermal instability of concrete, phenomenon commonly called spalling [1,2]. Concrete spalling consists in the detaching of fragments of the exposed surface and can seriously jeopardize the integrity of the whole structure (steel reinforcement directly exposed to fire, increase of the buckling risk of compressed elements, loss of insulating properties …). Nowadays, concrete spalling is still a phenomenon not well explained and which risk is not predictable by models. Spalling risk is commonly explained by two different mechanisms:

- Thermomechanical process: the heating of a concrete element involves high temperature gradients, particularly in the first centimetres of the heated surface. These gradients can be very important in the case of a rapid heating (e.g. for a fire) and induce high compressive stresses close to the heated surface. These stresses can locally overtake the concrete strength and cause the ejection of pieces [3–6].
- Thermo-hygral process: the heating of a concrete element involves mass transport into the porous medium. Fluids that are present into concrete (free water, water vapour, and dry air) are moving due to pressure and molar concentration gradients (Darcy and Fick laws). Particularly, fluids are moving through the inner zones of concrete. Since these zones are colder, water vapour starts to condensate and a "moisture clog" is gradually created close to the heated surface. This clog is assumed to be a region of concrete with high water content. Since this clog acts like a real barrier to fluid's flow, pore pressures are increasing [7]. These pressures can locally overtake the tensile strength of concrete and initiate the spalling [8–10].

Recent progresses in mathematical and numerical tools allow researchers to couple the two previous processes thanks to the use of

* Corresponding author. LaSAGeC², UFR Sciences et Techniques de la Côte Basque, Allée du Parc Montaury, 64600 Anglet, France.
*E-mail addresses:* jean-christophe.mindeguia@univ-pau.fr (J.-C. Mindeguia), pierre.pimienta@cstb.fr (P. Pimienta), albert.noumowe@u-cergy.fr (A. Noumowé), inokanema@msn.com (M. Kanema).

0008-8846/$ – see front matter © 2009 Elsevier Ltd. All rights reserved.
doi:10.1016/j.cemconres.2009.10.011

Thermo-Hydro-Mechanical models (THM modelling) [11–13]. Even so, spalling risk is still not easily predictable since the criterion of instability is unknown. On the other hand, we know from the literature that spalling can be observed in very different conditions: at very low heating rate (around 1 °C/min), cylindrical concrete samples can violently explode ([14], [15]) whereas for high heating rate (like a fire), spalling can look like a progressive peeling of the heated surface [16].

Among the key parameters that seem to explain spalling, the transport properties of concrete (permeability, porosity, water content, and damage) seem to be very important. In particular, we have to study how vapour pressures can build-up into concrete pore microstructure. This study focused particularly on the influence of the matrix compactness. We tested five concrete mixtures, with a constant aggregate volume but with different Water/Cement ratios.

## 2. Experimental details

### 2.1. Concrete mixes

In order to obtain different matrix compactness, the five concrete mixes were designed by varying the W/C ratio. The studied concrete mixes and some of their characteristics are given in Table 1. The compressive strength was measured at 28 days on water stored cylindrical samples. The permeability was assessed according to the CEMBUREAU method [17], based on the Klinkenberg approach [18]. The initial water content was assessed by drying cylindrical samples (Ø 150 mm × 50 mm) of the five different concretes at 80 °C (during 30 days). This water content refers to the initial free water of the sample. Other high temperature properties of these mixes were already assessed [11,19]. We note that the designed B450 and the B500 concrete mixes have a compressive strength higher than 60 MPa and can then be considered as High Performance Concretes. Moreover, we note that the B325 and the B350 concrete mixes have very similar properties at room temperature (the same permeability and initial free water content and almost the same compressive strength). We assume that the W/C ratio of the B325 was too high to see an important difference with the B350.

### 2.2. Setup

The experimental device developed by Kalifa et al. [9] was used. The test consists in applying a thermal load to one face of a prismatic sample ($30 \times 30 \times 12$ cm$^3$) using a radiant heater placed 3 cm above it. The sample lateral faces are insulated with porous ceramic blocks such as the thermal load can be assumed to be quasi-unidirectional.

The sample is placed on a balance in order to measure its mass loss during heating. The mass loss of the sample during heating is mainly due to the fluid's escape from concrete (water, vapour and dry air). Since the sample is unsealed, fluids can escape from all the sides of the sample. We want to emphasize that the mass loss measurement is then only specific to our testing conditions (sample geometry and heating). However, since the boundary conditions are the same for each test, we can use the mass loss measurement to compare the thermo-hygral behaviour of the five concretes. Moreover, mass loss measurement is a useful data for the validation of numerical models. The balance is placed under an insulating panel of rockwool to ensure that it is not sensitive to heating. Holes are made in the rockwool panel to not interfere with the weighing.

For simultaneous pore pressure and temperature measurements, samples were equipped during casting with gauges. These gauges are made of a sintered metal round plate (Ø $12 \times 1$ mm). The plate is welded to a thin metal tube (inner diameter 1.6 mm), which comes out of the unheated face of the sample. The tube is then connected to a piezo-electrical transducer thanks to a flexible tube filled with silicon oil. Secondly, thermocouples (Ø 1.5 mm) are introduced into the metal tubes down to the metal plate.

Samples were equipped with six gauges. One of them consists in a single plain tube in which one end is placed at 2 mm of the heated surface for only temperature measurement. In order to measure internal temperature and pressure, the other five gauges were placed at 10, 20, 30, 40 and 50 mm of the heated surface (Fig. 1). The six gauges are placed at the centre of the heated surface, in a $10 \times 10$ cm² square (Fig. 1). By this way, we assume that the pressure and temperature measurement are not influenced by the boundary conditions of the sample. Moreover, in this measurement zone, heating flow and fluid movement are assumed to be unidirectional.

### 2.3. Precisions about the pressure measurement

Concrete is a porous material, partially saturated by liquid water. Three phases fill the porous media: liquid water (free and adsorbed water), vapour and dry air. The interface between the liquid water and the gas phase (vapour and dry air) is characterized by a surface tension that induces a discontinuity between the fluids pressures. Particularly, the difference between liquid water pressure and gas pressure (defined as the sum of vapour pressure and dry air pressure) is called capillary pressure [20]. The capillary pressure mainly depends on the relative humidity of concrete pores and can reach high negative values (for instance, at 20 °C and for a relative humidity of 50%, the capillary pressure equals to −95 MPa [21]). One important result is that drying of concrete involves a decrease of capillary pressure, and can explain the delayed strains of concrete (such as drying shrinkage and creep) [21].

On the other hand, we assume that the introduction of one of our gauges (see Section 2.2) into concrete sample modifies its porous media. Indeed, we assume that a spherical zone of pressure measurement (6 mm of radius) is formed around the sintered metal round plate of a gauge (Fig. 2). We estimate the gas volume that is included in this spherical measuring zone at 50 mm$^3$ (10% of porosity, 50% of water saturation concrete), while the free volume in one gauge is equal to 130 mm$^3$. The sum of the spherical measurement zone gas volume and free volume of the gauge constitutes then an important free volume. During heating, we assume that only water vaporization is able to fill this important free volume, thanks to its important volume increase. Indeed, a simple temperature–volume phase diagram of water shows that the volume increase of vaporization

**Table 1**
Mixture proportions (kg), compressive strength, permeability and initial free water content of the tested concrete mixtures.

| | B325 | B350 | B400 | B450 | B500 |
|---|---|---|---|---|---|
| CEM I 52.5 cement | 325 | 350 | 400 | 450 | 500 |
| Siliceous 10/20 gravel | 960 | 960 | 960 | 960 | 960 |
| Siliceous 5/10 gravel | 89 | 89 | 89 | 89 | 89 |
| Siliceous 0/5 sand | 740 | 740 | 740 | 740 | 740 |
| Water | 202 | 194 | 177 | 160 | 143 |
| Superplasticizer | 0 | 0.35 | 1.04 | 1.73 | 2.43 |
| W/C ratio | 0.62 | 0.55 | 0.44 | 0.36 | 0.29 |
| 28 days compressive strength (MPa) | 35 | 36 | 53 | 62 | 76 |
| Permeability (m²) | $1.5 \cdot 10^{-16}$ | $1.5 \cdot 10^{-16}$ | $3.9 \cdot 10^{-17}$ | $1.2 \cdot 10^{-18}$ | $1.6 \cdot 10^{-20}$ |
| Initial free water content (%) | 3.8 | 3.8 | 3.5 | 3.2 | 2.8 |

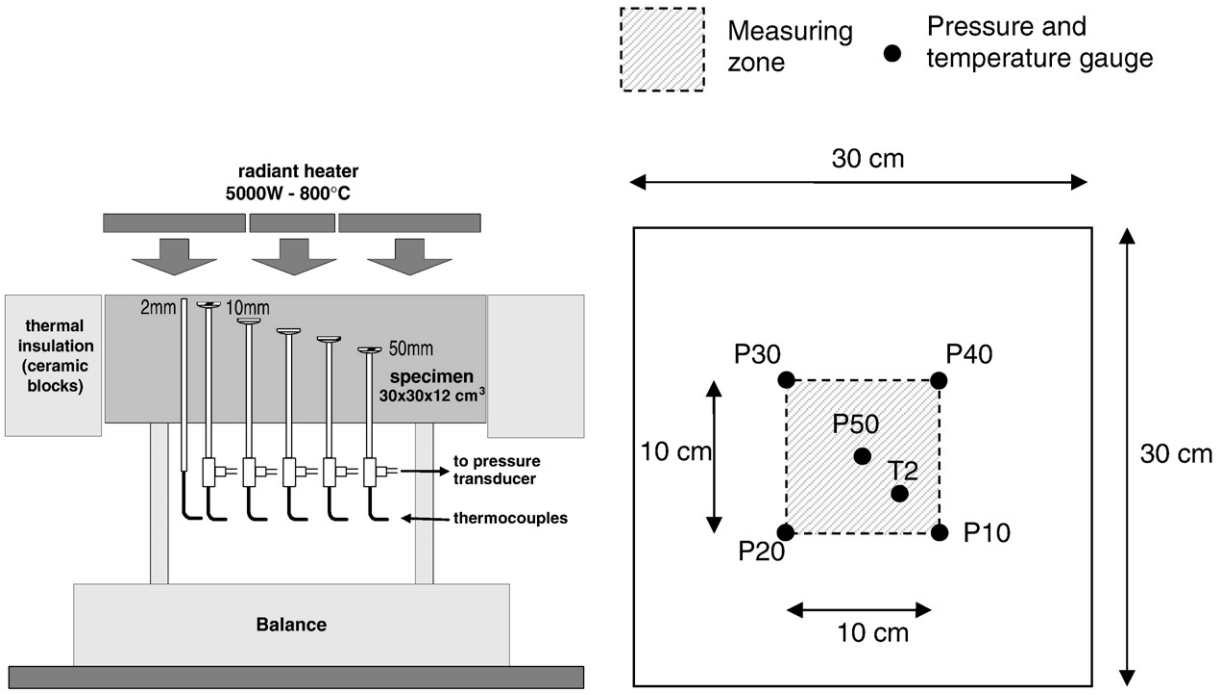


**Fig. 1.** Scheme of the experimental set-up (left). Right: position of the temperature and pore vapour pressure measuring zone (view of the heated surface of the sample).

process is quite more important than the thermal expansion of liquid water [22]. If we neglect the thermal expansion of dry air, we finally assume that our measurement system is theoretically only able to measure pore vapour pressure. However, we will discuss later in this paper about the contribution of dry air thermal expansion.

At last, since the measuring tubes are placed in the colder zones of the sample (Fig. 1) and since the flexible tubes that are filled with silicon oil are placed outside of the sample (Fig. 1), we assume that we do not need any calibration of the system regarding to the temperature increase.

### 2.4. Heating procedure

Two tests were carried out for each concrete mixture. The radiant heater was controlled in such a way that its temperature rapidly reaches 600 °C (after around 5 min). The power was then maintained constant during 6 h. At last, samples were naturally cooled down. The choice of the heating procedure was a compromise: fast enough to involve pore vapour pressure but slow enough to not induce too much thermal damage to the concrete sample. We present on Fig. 3 the temperature measured at 2 mm of the heated surface as well as the heating rate at this depth for one of the concrete mixtures (representative result for all the tests). We also present in this figure the temperature at 2 mm in a concrete sample during a fire test (ISO 834 curve). We can see that the heating scenario used in our study is relatively slow in comparison to a more realistic fire curve (like the ISO curve).

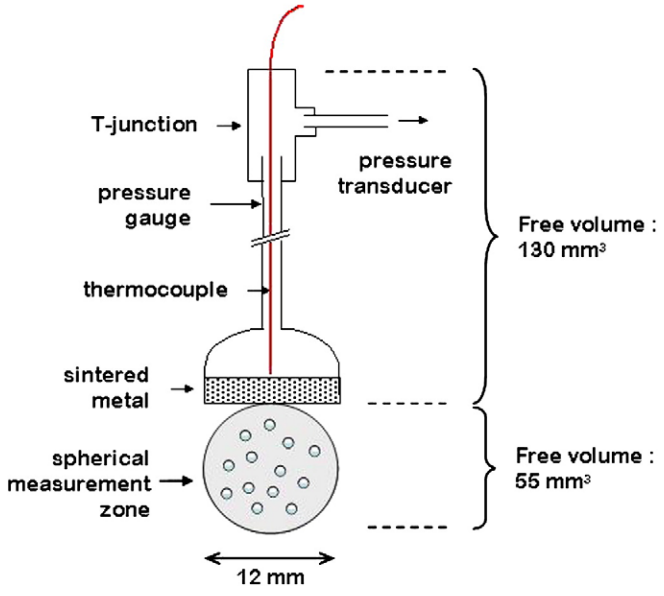


**Fig. 2.** Illustration of the spherical measuring zone that forms around a pressure gauge. Estimation of the free volume of the measuring system.

## 3. Results and analysis

### 3.1. Experimental observations

During the test, we observed water drops and vapour flow escaping from the samples. Moreover, severe damage of the samples was observed. These two observations had not been reported in previous tests carried out on other types of concrete [9]. We can see in Fig. 4 the cracking and the aggregate surface spalling of a sample after a test. This important damage (i.e. cracking and aggregate spalling) can be explained by the instable behaviour at high temperature of the flint aggregates used in the concrete mixtures. Complementary high temperature tests were carried out on flint aggregates (without cement paste). They confirmed the fact that the flint aggregates used in the concrete mixtures are thermally unstable from 120 °C to 200 °C. This behaviour is explained by the high temperature cleavage of flint, which can be due to high vapour pressures that build up into the own laminar microstructure of the aggregate [23].

### 3.2. Mass loss

We present on Table 2 the total water content (free+bonded water) before heating for the different mixtures in percentage. This value is the ratio between the mass of water introduced during the casting and the total mass of the components (cement, aggregates, water and superplasticizer). Table 2 also presents the proportion of

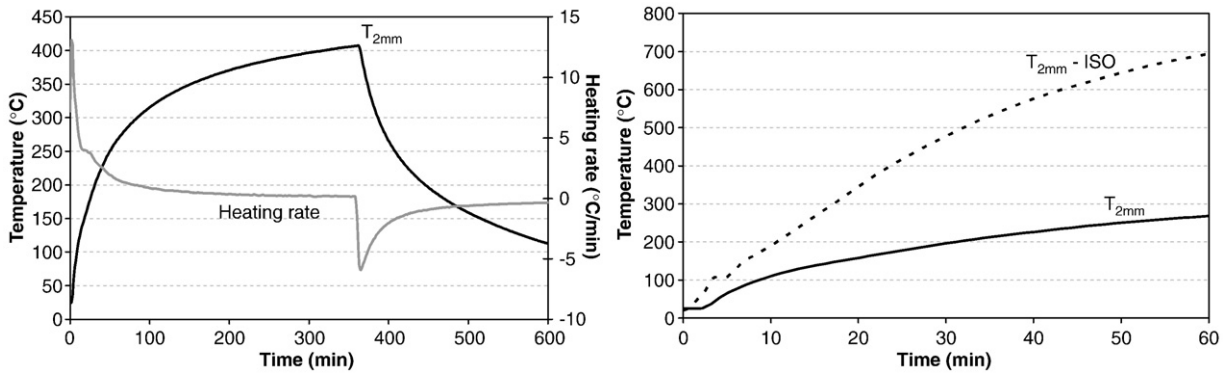


**Fig. 3.** Measured temperature and corresponding heating rate at 2 mm of the heated surface (left). Comparison with the temperature measured at 2 mm during the first 60 min of an ISO curve fire test (right).

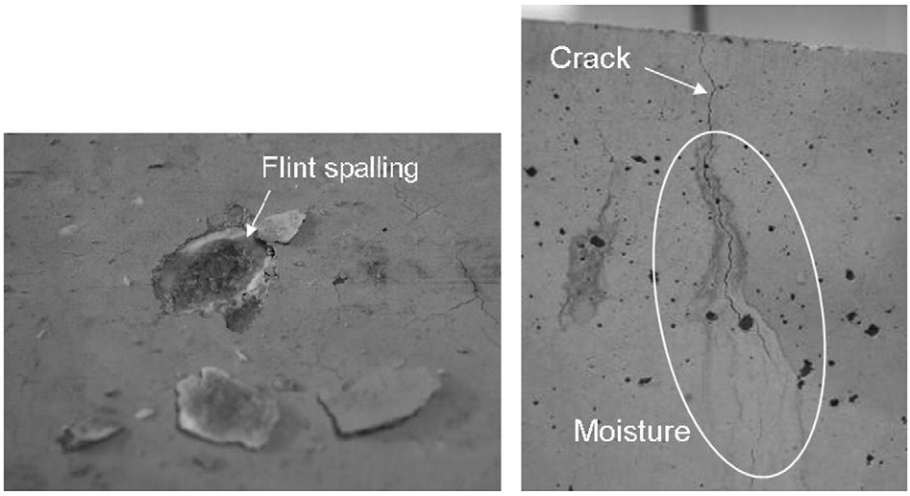


**Fig. 4.** Aggregate (flint) spalling on the heated surface (left). Cracking and moisture marks on the lateral face (right).

lost water after heating (ratio between the mass loss and the initial mass of the sample). Thanks to these two values, we can assess the ratio of water that has been extracted from the five concretes during heating. We can observe that the five concretes lose around two thirds of their initial water content. It means that after heating, one third of the water that had been introduced during casting is still present into concrete. Indeed, due to the relative low value of temperature into the samples during the tests (less than 400 °C on the exposed side and less than 160 °C on the unexposed side), concrete is not totally dried. Particularly, the chemically linked water cannot be totally removed as the entire dehydration of CSH and Portlandite is reached for higher temperature. But subtracting the initial free water content to the lost water, we can assess the quantity of chemically linked water that is released during the heating. The values are presented in the Table 2. We observe that the quantity of chemically linked water that is released during heating is weak regarding to the free water content of the sample (see Table 1). According to [26], this weak quantity of chemically linked water does not allow to amplify the built up of pore vapour pressure. We can see that the B325 has a weak ratio of extracted water in comparison with the B500. This can be explained by the fact that due to its high permeability, the B325 concrete loses more water during the storing period than the more compact concretes.

Fig. 5 presents the mass loss rate for the five concrete mixtures. The curves correspond to the average value of two tests for each type of concrete. Very few dispersion has been observed between the two tests (less than 5% of dispersion around the average value of mass loss rate). We note that the rate of water escape increases with the W/C ratio. Indeed, the low compactness of the concrete with high W/C ratio induces a higher fluid permeability and then makes easier the water escape.

**Table 2**
Total water content, lost water, relative lost water (lost water/total water) and released chemically linked water for the tested concrete mixtures.

| | B325 | B350 | B400 | B450 | B500 |
|---|---|---|---|---|---|
| Total water content (%) | 8.72 | 8.32 | 7.50 | 6.67 | 5.88 |
| Lost water (%) | 5.17 | 5.43 | 4.67 | 4.37 | 3.89 |
| Relative lost water (%) | 59 | 65 | 62 | 66 | 66 |
| Released chemically linked water (%) | 1.37 | 1.63 | 1.17 | 1.17 | 1.09 |

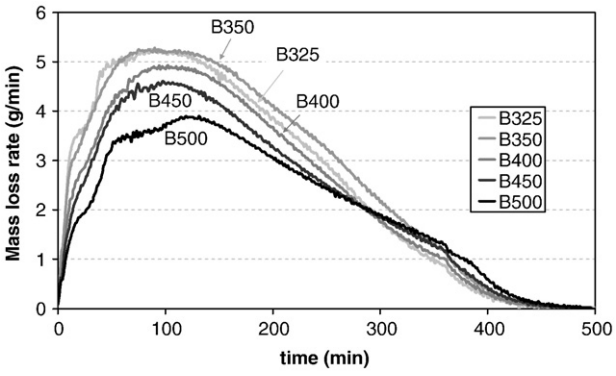


**Fig. 5.** Mass loss rate for the tested concrete mixtures.

### 3.3. Temperature

Fig. 6 presents the temperatures measured into the different concrete samples. For several tests, some gauges were unintentionally clogged with cement paste during casting. As a consequence, temperature measurements for some depths do not appear in the graphs.

For all concrete mixtures and for each measuring point, we observe a slight plateau, i.e. a perturbation, in the increase of temperature. This plateau is due to the water phase change (vaporization). This transformation is endothermic and then consumes a great part of the energy that is brought by heating. As a consequence, the heat transfer into concrete sample is slowed down. We want to emphasize that by this way, the water vaporization can induce additional temperature gradients. We will see in the last paragraph, that these gradients could modify the stresses in a concrete structure during fire. It was also observed that the temperature plateau depends on the concrete compactness. Indeed, it takes place at around 100 °C for the B325 and at around 175 °C for the B500. This dependence can be explained by the capillary forces that exist in a pore at the interface between liquid water, gas phase (vapour and dry air) and solid (concrete matrix). These capillary forces influence the vaporization process: under a pressure of 0.1 MPa, and for an infinite flat surface of water, vaporization takes place at 100 °C. At the opposite, for very small pores, capillary forces reaches high values and higher temperature is needed to extract vapour molecules from liquid water. In the case of concrete, the smaller the pore radius (i.e. the denser the concrete), the higher the vaporization temperature. The fact that vaporization takes place at around 100 °C in the less dense concrete (B325) indicates that capillary forces in these pores are not important, i.e. pore radius is high (probably due to cracking).

Thermal flow is quite similar between the five concrete mixtures. Indeed, we observe that the curves of temperature evolution are identical from one to another concrete (Fig. 6). For example, the temperature at 10 mm at the end of heating reaches around 350 °C for the five concretes, and the temperature at 50 mm reaches around 250 °C for the five concretes. This result shows that concrete thermal properties are not significantly influenced by the compactness of the material. According to the literature, thermal diffusivity of concrete is mainly controlled by the aggregate's nature, because of their important volume in concrete [24]. Since the aggregates are of the same nature and that their content is very close in the five concretes, it certainly explains why the temperature curves are very close from one to another concrete.

### 3.4. Pore pressure

Fig. 7 presents the pore pressure measured into the samples for all the tested concrete mixtures. When comparing two similar tests, we

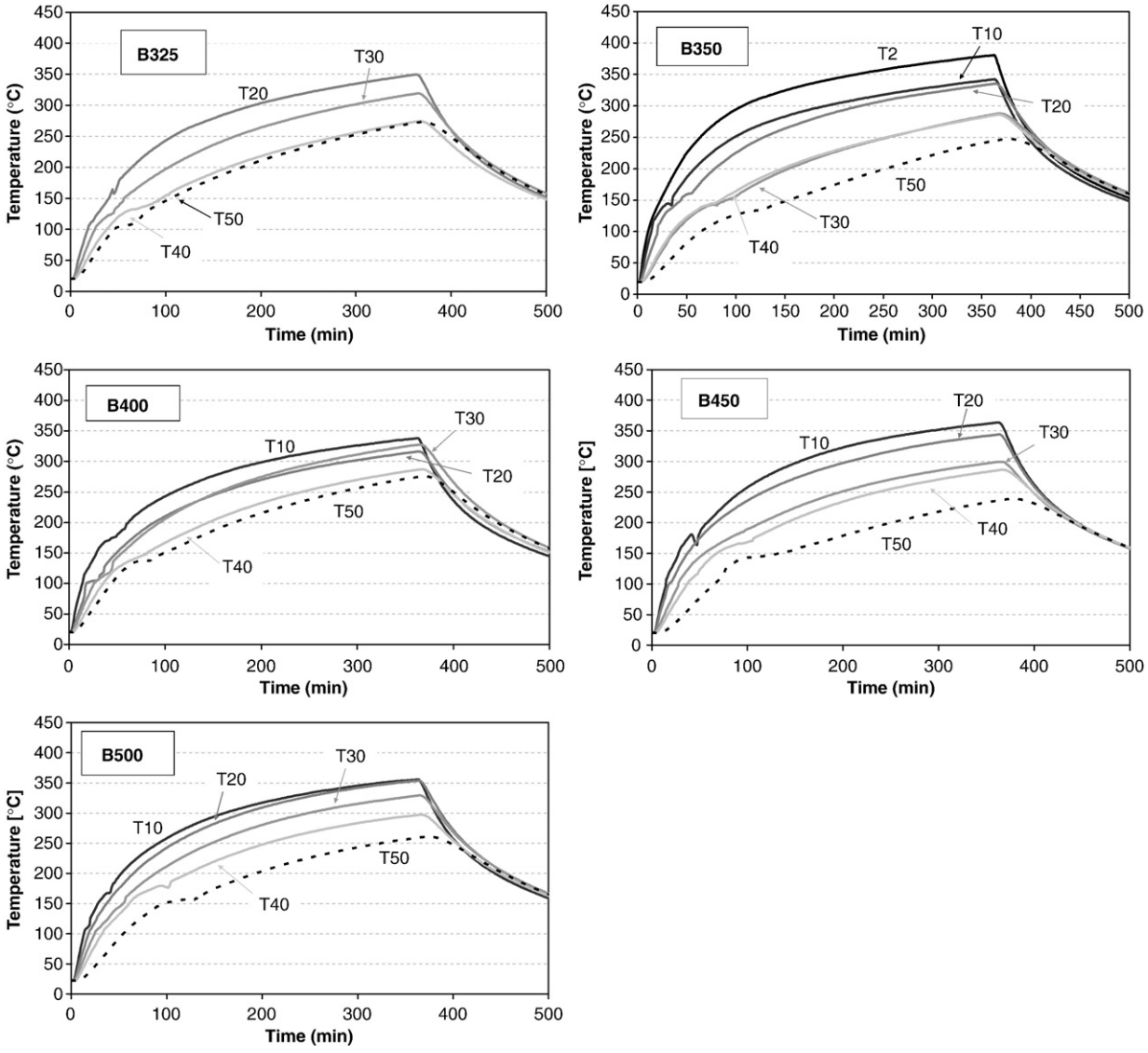


**Fig. 6.** Temperature as a function of time for all the tested concrete mixtures (the number after *T* is the distance in mm from the heated surface).

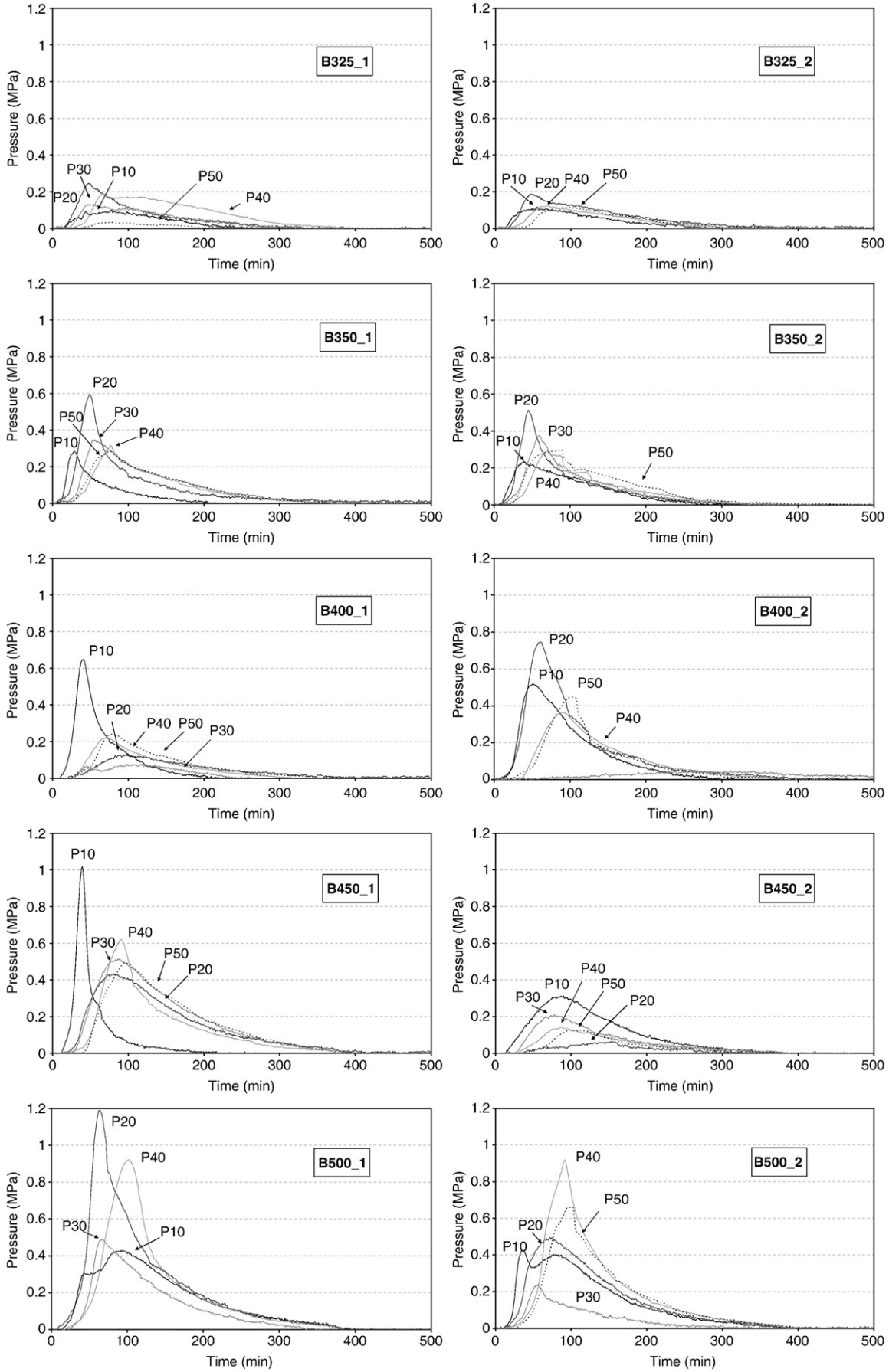


**Fig. 7.** Pressure as a function of time for all the tested concrete mixtures (the number after *P* is the distance in mm from the heated surface).

can see that the pressure measurement is scattered. It is a local measurement (see Section 2.2) and the pressure value depends on the tube location (into cement paste, close to an aggregate or in an air void). However, we can clearly see in Fig. 8 that the higher the W/C ratio, the lower the pore pressure (in this figure, we have assumed that the more representative value of pressure for each type of concrete is the highest measured value). This underlines the role of the concrete transport properties (porosity, permeability) on the thermo-hygral behaviour of the material, and in particular on the build-up of pore pressures [13].

We present in Fig. 9 the evolution of temperature and pressure as a function of time that have been measured at 40 mm of the exposed surface for one of the five concretes (the same behaviour has been observed for all the concretes). We can see that the peak of the measured pore pressure is reached during the temperature range of vaporization (slight plateau on the temperature curve). This result indicates that water vaporization into concrete is well assumed to be responsible for the build-up of the pore pressure that is measured by our experimental device. The diffusion of heat into concrete, and the complex hygral behaviour which is induced, may create a saturated zone close to the exposed surface (the so-called moisture clog). According to numerical results [11,13], this clog is generally created in a zone from around 1 cm to 6 cm from the exposed surface and its position depends on the transport properties of the concrete. As the vapour flow cannot go through the clog, it only goes towards the exposed surface (i.e. in the opposite direction of the heat flow). Moreover, the concrete located between the exposed surface and the moisture clog continues to dry and dehydrate. As soon as the rate of vapour escaping a pore (due to the flow towards the exposed surface) is higher than the rate of vapour filling the pore (coming from drying, dehydration and transport), the pressure starts decreasing. Simultaneously, by creating more available volume in the matrix, and especially by increasing the permeability of the material to vapour escape [27], cracking can also contribute to the pore pressure decrease [3]. These two phenomena can explain the bell shape of the pressure curves.

In Fig. 10, the evolution of the pore pressure as a function of temperature is presented. Experimental results of pressure (P) are compared with the saturating vapour pressure curve ($P_{vs}$). For many cases, it can be observed that measured pressures follow the $P_{vs}$ curve during the ascending branch. This result seems to confirm that the pore pressure that is measured by our experimental device is vapour pressure. However, for some results, the measured pressures are higher than the $P_{vs}$. Since it is theoretically impossible, vapour pressure is not responsible for this overpressure. This overpressure is often attributed to the partial pressure of the dry air that is enclosed in the porous media [9,25]. The partial pressure of air in a pore is strongly dependent on its liquid water saturation: the higher the water saturation, the lower is the free volume available to the air to expand during heating. As a consequence, for pores with high liquid water content, the contribution of thermal expansion of dry air to the total pressure will be important.

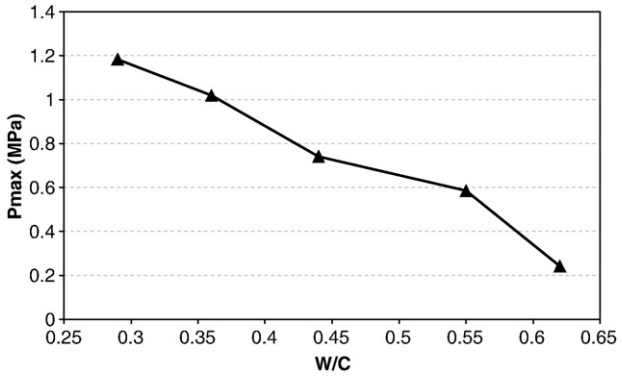


**Fig. 8.** Maximum pressure as a function of W/C ratio for all tests.

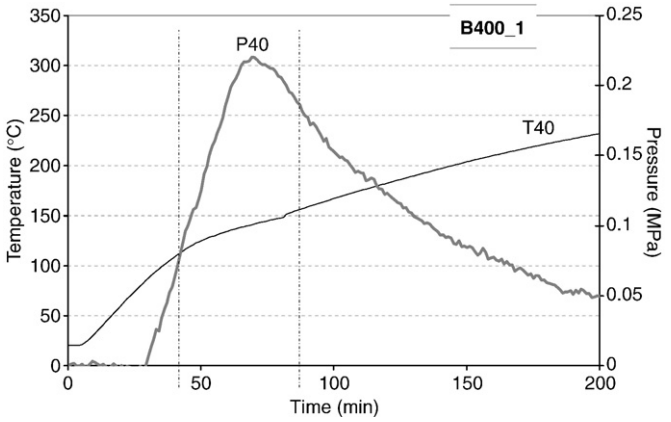


**Fig. 9.** Evolution with time of the temperature and pore pressure measured at 40 mm of the exposed surface for one of the five concretes. It must be noticed that the scales for pore pressure are different in the graph.

On the other hand, since we assume that during heating, water is moving to the inner part of the sample (transport that may create a moisture clog), it can explain why the overpressure is more important in the deepest zones from the heated surface of the sample (see Fig. 10). In Fig. 10, we also observe that P10 that was measured in B450 shows a different behaviour than the other sensors. It is attributed to the original evolution of the temperature that was measured at 10 mm in the B450 (see Fig. 6). Indeed, we observe around 175 °C (i.e. for the temperature corresponding to the P10 highest value), a decrease of the temperature (around 20 °C of cooling). This phenomenon can be due to a very important consummation of energy by the phase transformation of water. This consummation is assumed to be responsible for the cooling of a concrete zone close to the sensor.

Furthermore, it was observed that the measured pore pressures vary approximately from 0.2 MPa (B325) to 1 MPa (B500). These pressures can be considered as low values compared to those of previous studies carried out on concrete with similar compactness [26]. This may be explained by the important damage (i.e. cracking) of the samples due to the unstable behaviour of the flint aggregates used in the concrete mixtures (see Section 3.1). Indeed, there is an important link between the permeability and the damage of concrete [27]. In particular, high damage strongly modifies the transport properties of concrete, making easier by this way the movement of fluids. This can be clearly seen in Fig. 11 where we compare the mass loss rate of the B350 and B400 concretes with the mass loss rate of similar concretes made with thermally stable aggregates (calcareous aggregates) [26]. Indeed, the maximal mass loss rate is higher for the cracked samples and the peak of mass loss (time for reaching the maximal rate) appears sooner. One of the consequences of this cracking induced by aggregate instability is the fact that it does not allow the build-up of important pressure. As a first conclusion, cracking must be taken into account in order to correctly deal with the thermo-hygral behaviour of concrete at high temperature. Particularly, in case of rapid heating (e.g. for a fire), concrete can be strongly damaged and pore vapour pressure should then be significantly reduced [26].

In this study, we did not measure high pore vapour pressure in the five concrete mixtures due to the cracking induced by the aggregate's thermal instability. On the other hand, previous heating tests showed that the risk of spalling exists for these five mixtures, and can even be very important for the densest ones [11]. From this observation and from the results presented in this paper, it can be deduced that pore pressures are not the only origin of spalling. Recent experimental studies from the authors [26] and from a Swedish laboratory [28,32] seem to confirm this assumption. However, despite of the fact that spalling risk cannot be explained only by pore pressures, it must be emphasised that the moisture content and the overall moisture

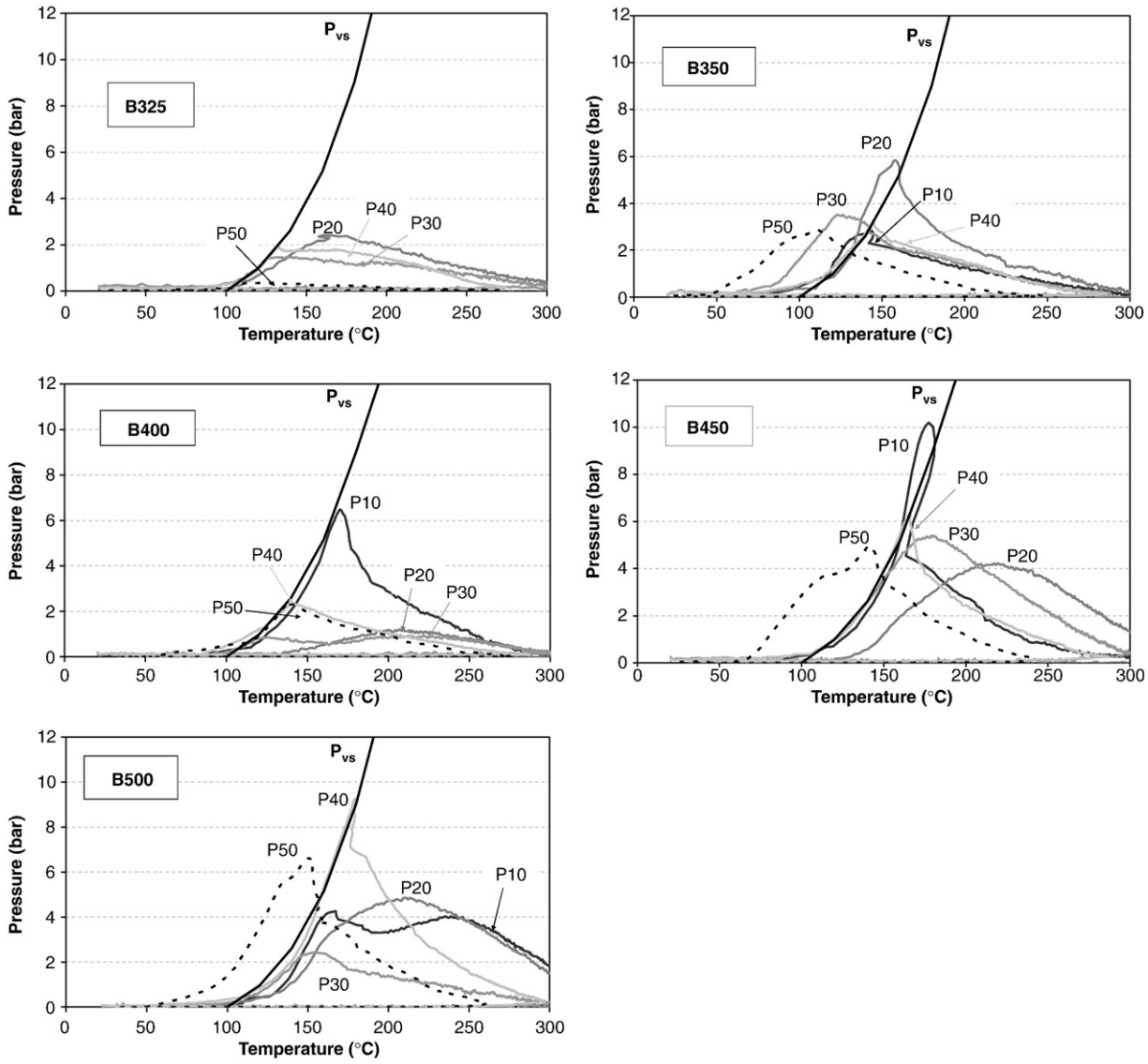


**Fig. 10.** Pressure as a function of temperature for the tested concrete mixtures, plotted together with the saturating vapour pressure curve ($P_{vs}$).

movement can play an important role for spalling. In particular, it has been observed in this study that the moisture content modifies the heat transfer into concrete and then induces additional thermal gradients. By using numerical simulations, we will see in the next paragraph how these thermal gradients can influence the mechanical behaviour of concrete during heating.

## 4. Numerical discussion

Following the experimental observations (see Section 3.3), the influence of the water vaporization on the behaviour of concrete during heating has to be analysed. Particularly, we want to see how the thermomechanical behaviour (elastic behaviour) of concrete can

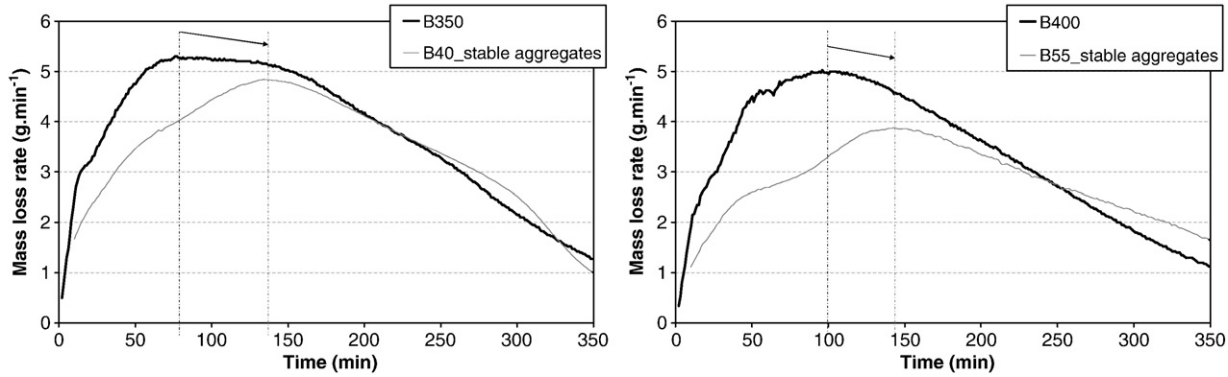


**Fig. 11.** Comparison of the mass loss rate between the B350 and the B400 mixtures and similar concretes made with thermally stable aggregates (B40 and B55, see [21]). The arrow underlines the time-lag of maximal mass loss rate between the two types of concrete.

**Table 3**
Boundary conditions for the thermomechanical simulation of a concrete wall during ISO-fire.

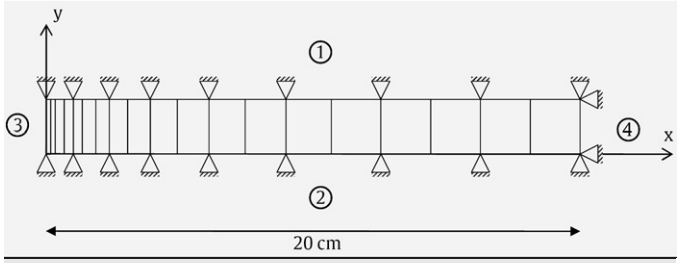


| Side | Variables | Values and coefficients |
|---|---|---|
| ①, ② | Displacement $u_y$ | $u_y = 0$ |
| | Thermal flow $q_T$ | $q_T = 0$ |
| ③ | Temperature $T$ | Convective–radiative with $h_c = 25$ (W/m$^2$K), $\varepsilon = 0.7$ |
| | | $T(t)$ according to the standard ISO-fire 834 |
| ④ | Displacement $u_x$ | $u_x = 0$ |
| | Temperature $T$ | Convective–radiative with $h_c = 4$ (W/m$^2$K), $\varepsilon = 0.7$ |
| | | $T = 293$ K |

**Table 4**
Concrete parameters used in the thermomechanical simulation.

| Parameters | | Values |
|---|---|---|
| Mechanical | Modulus of elasticity | 52 GPa at room temperature, see Fig. 12 for the evolution with temperature |
| | Poisson coefficient | 0.25 |
| | Thermal expansion coefficient | 1.5 $10^{-5}$K$^{-1}$ |
| Thermal | Thermal conductivity | 1 W.m$^{-1}$.K$^{-1}$ |
| | Bulk density | 2300 kg.m$^{-3}$ |
| | Specific heat | See Fig. 12 for the evolution with temperature |

be modified because of the phase transformation of water. This will allow us to give new tracks of investigation to assess the possible causes of thermal spalling of concrete.

In this chapter, thermomechanical behaviour of a concrete wall exposed to ISO-fire will be analysed. A finite-element software has been used (Cast3m). The boundary conditions are schematically presented in Table 3 and concrete properties are given in Table 4. Among the parameters, the assumed evolution of the modulus of elasticity with temperature is given in Fig. 12. Modulus of elasticity is assumed to decrease with heating in order to implicitly take into account the thermal damage of concrete. This behaviour is often experimentally assessed [29]. The water content of the wall, and thus its potential for water vaporization, is implicitly taken into account by varying the peak of specific heat between 100 °C and 250 °C. This approach takes inspiration from the Eurocode 2, Part 1.2 [30]. We simulated the elastic thermomechanical behaviour of the concrete wall with three different levels of water content (i.e. three different levels of vaporization potential): constant specific heat (no vaporization potential), a peak of 5000 Jkg$^{-1}$K$^{-1}$ (middle vaporization potential) and a peak of 10,000 Jkg$^{-1}$K$^{-1}$ (high vaporization potential). The three different evolutions of specific heat are given in Fig. 12.

Fig. 13 presents the results of the thermal simulations. In this figure, we note that the higher the water content (i.e. the higher the peak of specific heat), the more important the slowing down of the heat flow. This result is in good accordance with the experimental results presented in Section 3.3. A consequence of the thermal slowing down is the increase of the thermal gradients close to the heated surface (i.e. in the zone of concrete spalling). This is clearly shown in the second plot of the Fig. 13 where we observe that the difference between the surface temperature and the temperature at 10 mm reaches the highest values for the higher water content simulation. In particular, the difference of temperature is particularly high during the period when one can assume that concrete spalling occurs during an ISO-fire.

Fig. 14 presents the results of the thermomechanical simulations. For each case of specific heat, we observe that a compressive clog is progressively created close to the heated surface. The formation of this clog is due to the progressive degradation of the concrete close to the heated surface (due to the decrease of the modulus of elasticity with heating) and may be a possible cause for concrete fracture close to the heated surface, i.e. a possible cause for concrete spalling. The influence of the water content, and particularly the influence of the vaporization process, is analysed on the Fig. 15. In this figure, we observe that the higher the vaporization potential, the closer to the heated surface the compressive clog. This result indicates that for high water content concretes, the fire-induced compressive zone is thinner. Inspired by [31], if we assume that spalling can be caused by the buckling of a concrete band close to the heated surface, our simulations show that the concrete buckling risk (i.e. spalling risk) is higher for high water content concrete. This assumption is currently observed during experiments [1,2,26] and it allows us to emphasize the possible link between concrete spalling and the thermomechanical process. In other words, our simulation shows that not only the water content of concrete play a role in the thermo-hygral process but also in the thermomechanical one.

## 5. Conclusions

Samples of five concrete mixtures were tested in order to study the influence of the matrix compactness on the concrete behaviour at

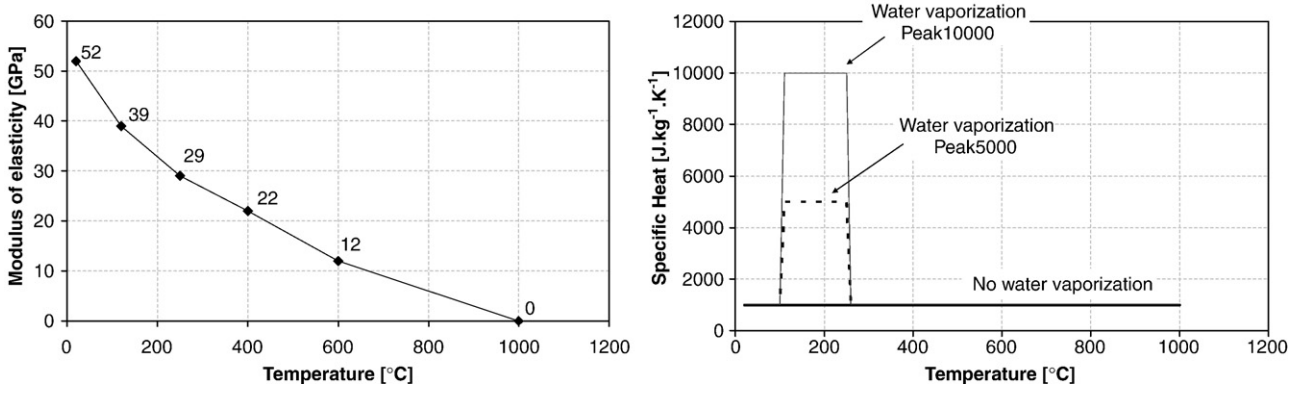


**Fig. 12.** Assumed evolution of concrete parameters with temperature: modulus of elasticity (left) and specific heat (right). Water vaporization is taken into account by varying the peak of specific heat between 100 °C and 250 °C.

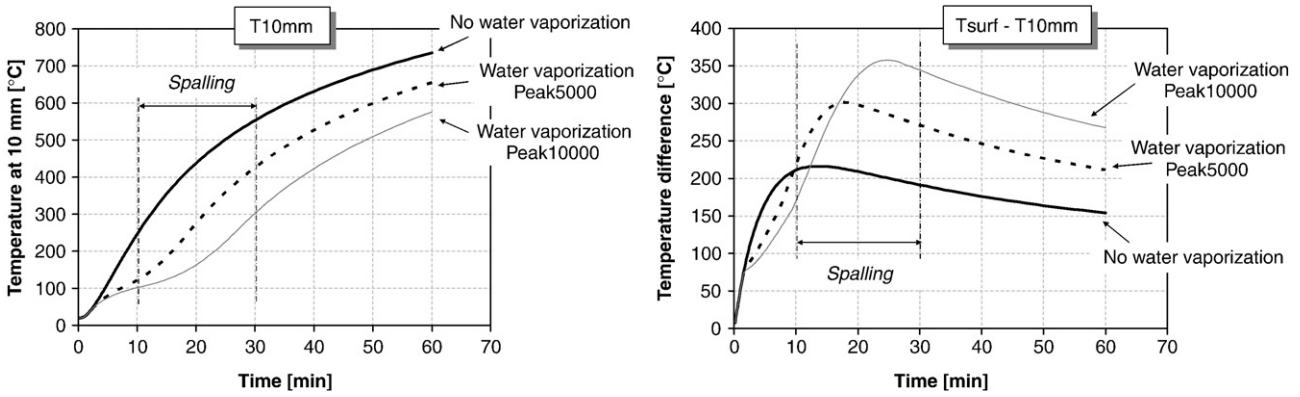


**Fig. 13.** Evolution of the temperature at 10 mm from the exposed surface depending on the peak of specific heat (left). Evolution with time of the difference between the temperature at the surface and the temperature at 10 mm depending on the peak of specific heat (right). Concrete spalling is assumed to occur between the 10th and the 30th min of ISO-fire.

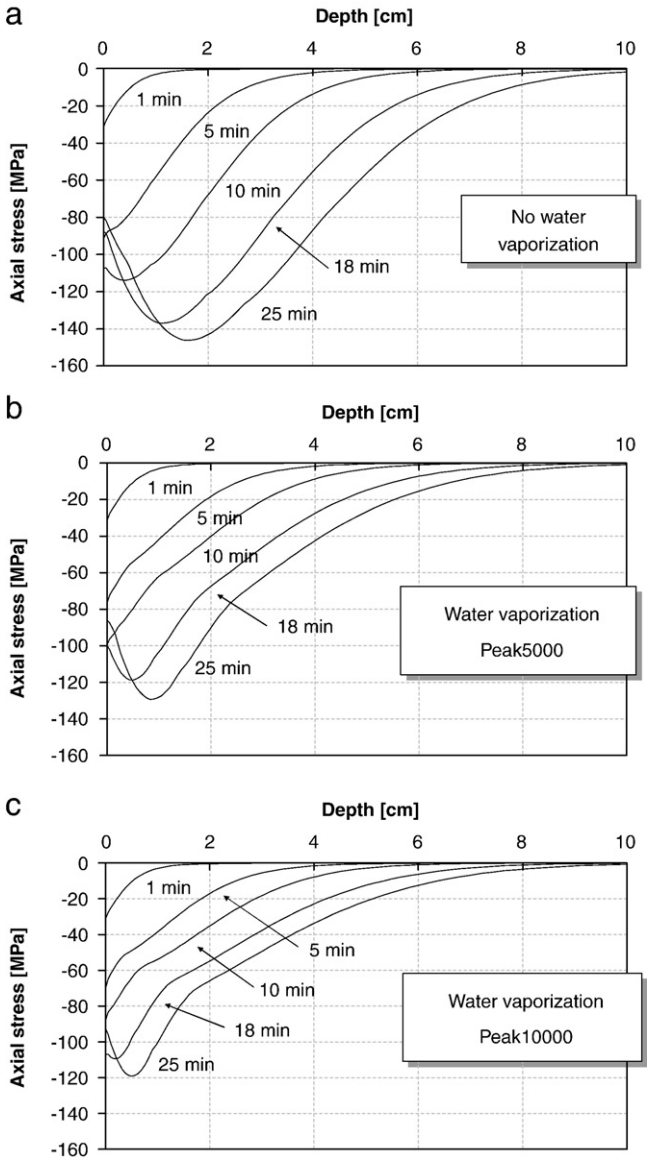


**Fig. 14.** Profile of the axial stress ($\sigma_{xx}$) at different times of heating: a—no water vaporization (no peak), b—water vaporization (peak of 5000 J.kg$^{-1}$.K$^{-1}$) and c— water vaporization (peak of 10,000 J.kg$^{-1}$.K$^{-1}$).

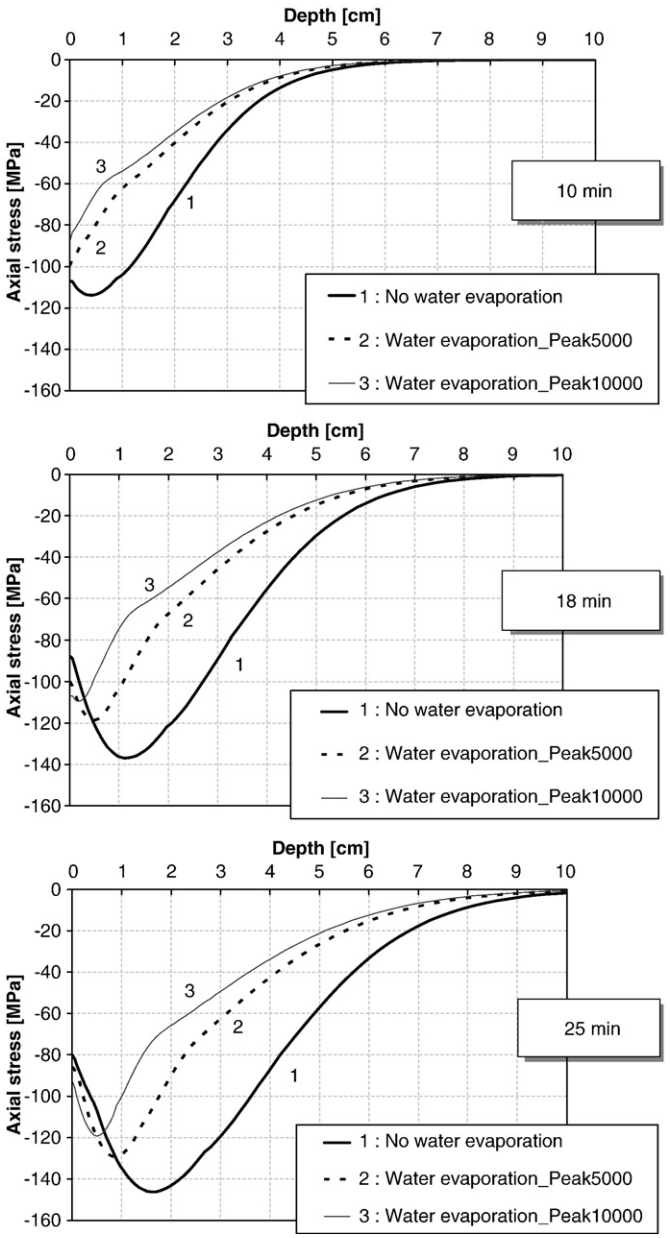


**Fig. 15.** Comparison of the axial stress ($\sigma_{xx}$) at 3 different times of heating depending on the peak of specific heat.

high temperature. The study focused on the temperature and pore vapour pressure fields that develop into concrete during heating as well as on the samples mass loss. The tests presented have been carried out at a heating rate lower than the one provided by the ISO curve (see Fig. 3). The results allow discussing about the physical origins of spalling. The following conclusions can be drawn.

The thermal instability of flint aggregates involves an important damage of the concrete samples. Some local spalling on the exposed surface was observed.

The permeability (or matrix compactness) of the concrete strongly influences the water escape during heating. Lower is the permeability and slower is the mass transfer into concrete. This is in good agreement with theoretical considerations such as the Darcy and Fick laws.

Pore pressure is built-up into concrete due to water vaporization. The maximal pressure strongly depends on the concrete compactness. In particular, low permeability involves high build-up of pore pressure.

The coupled heat and mass transfers into concrete involve the development of a saturation front (also called moisture clog). In zones of quasi water-filled pores, the thermal expansion of dry air induces some overpressure.

In comparison to previous studies, it has been observed that the concrete cracking (caused by the thermal instability of aggregates) strongly limits the build-up of pressure. However, another study has shown that the five tested concretes present an important risk of spalling. It appears then that the pore vapour pressures are not the only cause to the concrete spalling risk. Another explanation for spalling risk can come from thermomechanical assumptions. In particular we observed in this study that the water vaporization modifies the heat transfer and the temperature profile into concrete. In particular, it can induce a decrease of internal heating rate involving additional thermal gradients. This phenomenon has been emphasised by a numerical simulation. The simulation showed that the water content of concrete can modify the thermomechanical behaviour of concrete during heating. In particular, the buckling risk of a concrete band close to the heated surface can be increased in high water content concretes. According to previous studies, since this buckling risk may be relied to spalling risk, our simulations showed the possible link between concrete spalling and the thermomechanical process.

More experimental tests will be carried out to confirm and to complete the different assumptions about the physical origins of spalling risk. Other fire tests (with ISO and Hydrocarbon Modified Curve) with pore vapour pressure measurement have also been carried out on other types of concretes [32]. The first results seem to confirm that pore vapour pressure build-up is not the only cause for spalling.

## Acknowledgements

More of the results obtained in this paper were obtained with the device developed by Dr Pierre Kalifa and Mr François-Dominique Menneteau of CSTB. The authors would like to acknowledge them for their help. Specials thanks are also given to Robert Jansson from SP, Sweden, for the quality of our discussions about spalling mechanisms.

## References

[1] V.K.R. Kodur, Spalling in high strength concrete exposed to fire — concerns, causes, critical parameters and cures, Proceedings of Structures Congress, Advanced Technology in Structural Engineering, Philadelphia, USA, May 8–10 2000.
[2] L. Bostrom, R. Jansson, Spalling of self compacting concrete, Proceedings of SIF'06 workshop, Structures in Fire, Aveiro, Portugal, May 2006.
[3] Z.P. Bažant, Analysis of pore pressure, thermal stress and fracture in rapidly heated concrete, Proceedings of the International workshop on fire performance of high-strength concrete, NIST, Gaithesburg, USA, 1997.
[4] F.J. Ulm, P. Acker, M. Lévy, The Chunnel fire. II: analysis of concrete damage, Journal of Engineering Mechanics 125 (1999) 283–289.
[5] Y. Msaad, G. Bonnet, Analysis of heated concrete spalling due to restrained thermal dilation: application to the Chunnel fire, Journal of Engineering Mechanics 132 (2006) 1124–1132.
[6] J. Sercombe, C. Gallé, S. Durand, P. Bouniol, On the importance of thermal gradients in the spalling of high-strength concrete, Proceedings of EM 2000: Fourteenth Engineering Mechanics conference, Austin Texas, USA, 2000.
[7] T.Z. Harmathy, Moisture in materials in relation to fire tests, Special Technical Publication, no 385, ASTM, 1964.
[8] Y. Anderberg, Spalling phenomena of HPC and OC, Proceedings of the International workshop on fire performance of high-strength concrete, NIST, Gaithesburg, USA, 1997.
[9] P. Kalifa, F.D. Menneteau, D. Quenard, Spalling and pore pressure in HPC at high temperature, Cement and Concrete Research 30 (2000) 1915–1927.
[10] S. Dal Pont, H. Colina, A. Dupas, A. Ehrlacher, An experimental relationship between complete liquid saturation and violent damage in concrete submitted to high temperature, Magazine of Concrete Research 57 (no 8) (2005) 455–461.
[11] M. Kanema, M.V.G. De Morais, A. Noumowe, J.L. Gallias, R. Cabrillac, Experimental and numerical studies of thermo-hydrous transfers in concrete exposed to high temperature, Heat and Mass Transfer 44 (N° 2) (2007).
[12] R.T. Tenchev, J.A. Purkiss, L.Y. Li, Numerical analysis of thermal spalling in a concrete column, Proceedings of the 9th National congress on theoretical and applied mechanics, Varna, Bulgaria, 2001.
[13] D. Gawin, F. Pesavento, B.A. Schrefler, Towards prediction of the thermal spalling risk through a multi phase porous media model of concrete, Computer Methods in Applied Mechanics and Engineering (n°195) (2006) 5707–5729.
[14] L.T. Phan, J.R. Lawson, F.L. Davis, Effects of elevated temperature exposure on heating characteristics, spalling, and residual properties of high performance concrete, Materials and Structures 34 (2001).
[15] A. Noumowe, H. Carré, A. Daoud, H. Toutanji, High-strength self-compacting concrete exposed to fire test, American Society of Civil Engineering Publications, ASCE Materials Journal 18 (N° 6) (2006).
[16] P. Kalifa, D. Pardon, F.D. Menneteau, C. Gallé, G. Chené, P. Pimienta, Comportement à haute température des bétons à hautes performances: de l'éclatement à la microstructure, Cahiers du CSTB, no 3154, 1999, (in French).
[17] J.J. Kollek, Mesure de la perméabilité du béton à l'oxygène par la méthode CEMBUREAU, Ciments, Plâtres, Chaux, vol. 778, pp 169–173, 1989.
[18] L.J. Klinkenberg, The permeability of porous media to liquids and gases, Drilling and Production Practice, 1941, pp. 200–231.
[19] M. Kanema, A. Noumowé, J.L. Gallias, R. Cabrillac, Propriétés mécaniques et perméabilité résiduelles de bétons exposés à une température élevée, Revue Européenne de Génie Civil 10 (no 10) (2006) (in French).
[20] B.A. Schrefler, G.A. Khoury, D. Gawin, C.E. Majorana, Thermo-hydro-mechanical modelling of high performance concrete at high temperatures, Engineering Computations 19 (7–8) (2002) 787–819.
[21] F. Benboudjema, F. Meftah, J.M. Torrenti, A viscoelastic approach for the assessment of the drying shrinkage behaviour of cementitious materials, Materials and Structures 40 (2) (2007) 163–174.
[22] CRC Handbook of Chemistry and Physics, 90th Edition, David Lide, National Institute of Standards & Technology, 2009.
[23] C. Meyer-Ottens, The question of spalling of concrete structural elements under fire loading, PhD Thesis, Technical University of Braunschweig, Germany, 1972.
[24] Z.P. Bazant, M.F. Kaplan, Concrete at High Temperatures: Material Properties and Mathematical Models, Longman, Harlow, 1996 516 pp.
[25] O. Kontani, S.P. Shah, Pore pressure in sealed concrete at sustained high temperatures, Proceedings of the International Conference On Concrete Under Severe conditions, CONSEC'95 Sapporo (Japan) 2 (1995) 1151–1162.
[26] J.C. Mindeguia, P. Pimienta, C. La Borderie, H. Carré, Experimental study of fire behaviour of different concretes — thermo-hygral and spalling analysis, Proceedings of the Fib workshop Fire design of concrete structures, Coimbra (Portugal), 2007.
[27] M. Choinska, A. Khelidj, G. Chatzigeorgiou, G. Pijaudier-Cabot, Effects and interactions of temperature and stress-level related damage on permeability of concrete, Cement and Concrete Research 37 (n 1) (January 2007) 79–88.
[28] R. Jansson, L. Boström, The influence of pressure in the pore system on fire spalling of concrete, Proceedings of the fifth international conference "Structures in Fire", Singapore, May 28–30 2008, pp. 418–429.
[29] I. Hager, P. Pimienta, Mechnical properties of HPC at high temperature. Fib task group 4.3 "Fire design of concrete structures". Milan, Italy, 2 – 4 December 2004.
[30] EN 1992-1-2, Eurocode 2: Design of concrete structures, Part 1.2 Structural fire design, December 2004.
[31] D. Gawin, F. Pesavento, B.A. Schrefler, Towards prediction of the thermal spalling risk through a multi-phase porous media model of concrete, Computer Methods in Applied Mechanics and Engineering 195 (41–43) (2006) 5707–5729.
[32] R. Jansson, L. Bostrom, The influence of pressure in the pore system on fire spalling of concrete, Fire Technology, Special issue on the SIF'08 conference, March 2009.